VOL. 11, NO. 8, APRIL 2016 ISSN 1819-6608
ARPN Journal of Engineering and Applied Sciences


www.arpnjournals.com

# THE EFFECTS OF THICKNESS ON BIOMECHANICAL BEHAVIOR OF ARTICULAR CARTILAGE: A FINITE ELEMENT ANALYSIS

Yusra Liyana Jaafar[1], Mohd Juzaila Abd Latif[1,2], Nur Hikmah Hashim[1] and Mohammed Rafiq Abd Kadir[3]
[1]Faculty of Mechanical Engineering, Universiti Teknikal Malaysia Melaka, Hang Tuah Jaya Durian Tunggal, Melaka, Malaysia
[2]Centre of Robotics and Industrial Automation, Universiti Teknikal Malaysia Melaka, Hang Tuah Jaya Durian Tunggal, Malaysia
[3]Faculty of Biomedical Engineering and Health Sciences, Universiti Teknologi Malaysia, Skudai, Johor, Malaysia

## ABSTRACT

It is important to study joint contact mechanics in order to understand the human joint function and degeneration. In previous studies, the cartilage behavior was investigated using computational method assuming the cartilage to be flat and an ideal thickness. But, this assumption may not appropriate because the joint is naturally curved and the cartilage thickness varies across the articular cartilage. In this study, finite element (FE) analysis was performed to investigate the effect of cartilage thickness on contact pressure and pore pressure of cartilage in indentation test. An axisymmetric FE model of cartilage was developed according to the thickness and radius measured in the experiment. The cartilage was modeled as biphasic material to describe the properties of cartilage. Based on the result, the lowest cartilage thickness of 0.3 mm thickness generated 48% higher in contact pressure and 59% higher in pore pressure, compared to the highest thickness cartilage. This could indicate that the cartilage thickness does affect the contact pressure and pore pressure.

**Keywords:** articular cartilage, finite element, thickness.

## INTRODUCTION

Osteoarthritis (OA) is the most frequent and symptomatic health problem for older and middle aged people. OA can occur at any synovial joint in human body, particularly at weight bearing joint such as knee, hips, spine and foot joints (Buckwalter and Martin, 2006). The early sign of OA includes limitation of movement in active joint (Buckwalter and Martin, 2006). The causes of OA is due to excessive of mechanical load, ligament derangements, cartilage degeneration, subchondral bone changes and muscular impairments (Egloff *et al.*, 2012). Degeneration of articular cartilage in synovial joints has long been recognized as the main source of OA (Tchetina, 2011), (Buckwalter and Martin, 2006). The damage of cartilage tissue initiates at the surface of cartilage and become porous and high in permeability, where the water content becomes more than 90% (Grenier *et al.* 2014). This leads to the decreased of modulus of elasticity and thus reduction in load bearing capability of the articular cartilage (Bhosale and Richardson 2008).

Articular cartilage consists of four different layers, which are superficial zone, transitional zone, middle zone and calcified zone. Superficial zone is the thinnest of all layers and the disruption of this area may lead to development of early stage of OA (Bhosale and Richardson, 2008). Articular cartilage has a unique structure and composition, which consists of two phases; fluid phase and solid phase. The percentage of water is higher in liquid phase, which is 68-85% of the cartilage weight (Kazemi *et al.*, 2013). The functions of cartilage are to support the joint and distribute the load for frictionless movement, reduce the contact stress and provide lubrication by synovial fluid (Sharma *et al.*, 2011), (Boschetti *et al.*, 2004), (Matsiko *et al.*, 2013), (Meng *et al.*, 2013). In addition, cartilage tissue varies in thickness and curvature, depending on the location in the body (Wu *et al.*, 1996).

Recent advancement in computational method has simulated the cartilage using biphasic constitutive material model (Abd Latif *et al.*, 2012), (Harris *et al.*, 2012). The biphasic characteristic is widely used to represent the cartilage since it able to model the fluid flow in cartilage. In biphasic theory, there are two important biomechanical properties of cartilage, which are elastic modulus and permeability. These properties are dependent on the contact pressure and pore pressure which associates with the rate of fluid flow of the tissue. These properties were characterized using indentation test with impermeable spherical indenter to obtain the cartilage deformation-time which subjected to 10% to 20% cartilage strain of the cartilage thickness until the displacement reach to equilibrium.

In previous studies, the investigation of cartilage behavior by using computational method assumed that the cartilage to be flat with uniform thickness (Latif *et al.*, 2013), (Choi and Zheng, 2005). However, this assumption may not appropriate, as the joint is naturally curved and varies in thickness (Li *et al.*, 2013), (Toyras *et al.*, 2001), (Shepherd and Seedhom, 1999). Thus, the aim of this study is to investigate the effect of cartilage thickness on contact pressure and pore pressure of the cartilage during indentation test using axisymmetric FE model. These findings could be used to study the behavior of articular cartilage in synovial joint in computational studies.

## METHODOLOGY

### Specimen preparation

Articular cartilage of humeral head from bovine was used in this study as shown in Figure-1. The specimens were obtained from Pusat Sembelihan Jasin, Melaka after being slaughtered within 24 hours. The specimens were kept moist using phosphate buffered saline (PBS) and stored in refrigerator prior testing within

24 hours. The cartilage surface was divided into four sections to determine the thickness.

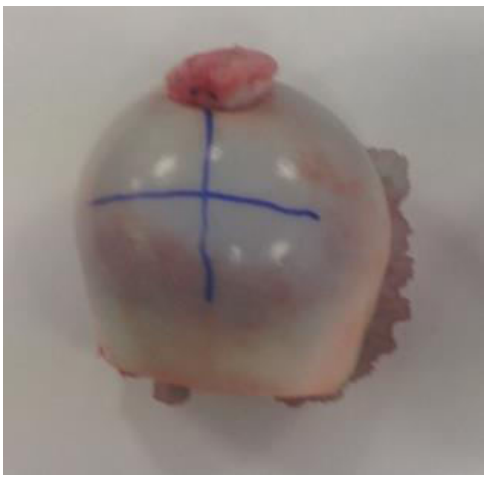

**Figure-1.** Cartilage specimen of humeral head.

**Cartilage thickness measurement**

The thickness of the cartilage for each point over the entire cartilage surface was measured using the test rig shown in Figure 2(a). A needle indenter was assembled with a shaft with total weight of 3.16 N load and then release to the points marked on the cartilage surface. The sharp needle pierced through to penetrate cartilage tissue and penetrate the cartilage until it reached the underlying bone. The displacement of the needle and the load response were captured to determine the cartilage thickness. This technique is frequently used in previous studies method to find the thickness of cartilage tissue (Abd Latif *et al.*, 2012), (Shepherd and Seedhom, 1999). The thickness measured in this experiment is within the range according to the previous studies as shown in Table-1.

**Table-1.** Thickness of normal articular cartilage in bovine synovial joints.

| Cartilage | Thickness, mm | Reference |
|---|---|---|
| **Humeral head (present)** | **0.3, 0.4, 0.5, 0.7** | **-** |
| Knee | 0.88±0.36 | (Jurvelin *et al.*, 1995) |
| Humeral head | 0.799-1.654 | (Toyras *et al.*, 2001) |
| Knee | 0.28±0.07 | (Danso *et al.*, 2014) |

**Cartilage curve measurement**

The curvature of the specimen was measured using profile projector as shown in Figure-2(b). The specimen was placed on the stage to produce the shadow on the projection screen. Then, several points at edge around of the specimen were captured to find the diameter of the humeral head.

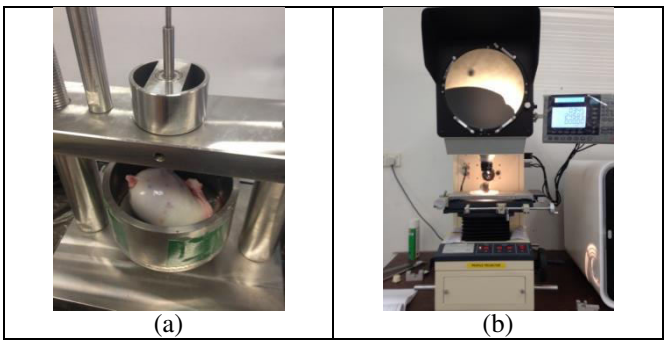


**Figure-2.** (a) Test rig for cartilage thickness measurement, (b) Cartilage curve measurement using profile projector

**Development of finite element model**

Articular cartilage and bone were modeled as an axisymmetric biphasic poroelastic using Abaqus software (Version 6.9). The cartilage was developed using the measured radius of 22.4 mm and measured thickness of 0.3 mm, 0.4 mm, 0.5 mm and 0.7 mm. The spherical indenter with 4 mm diameter was modeled as analytical rigid.

The element type for cartilage was set as four-node bilinear displacement and pore pressure elements (CAX4P). While, four-node bilinear elastic elements (CAX4) were used to represent the underlying bone (Latif *et al.*, 2013). Boundary and interface conditions were applied on the cartilage and indenter to replicate the experimental creep indentation test set up (Latif *et al.* 2013). The spherical indenter was only allowed to move in y-axis while the x-axis and rotational movement were constrained. As can be seen in the Figure 3, a contact-dependent flow condition was applied at the top surface of the cartilage. This was implemented at each increment such that flow was prevented only in the region when in contact with the cartilage surface. The model was verified and generated good agreement with previous study (Pawaskar, 2010). The material properties applied to the finite element models shown in Table-2.

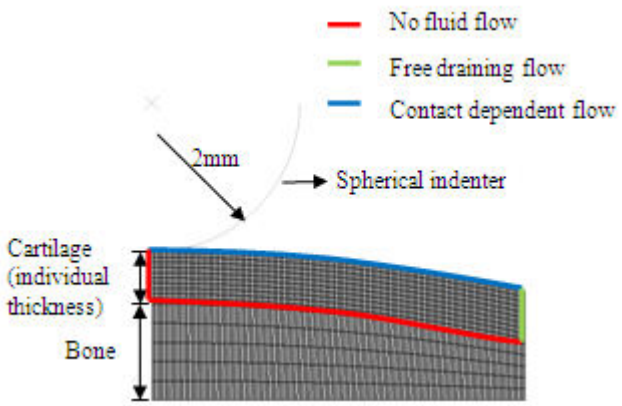


**Figure-3.** Axisymmetric FE model of curved-surface cartilage with flow boundary condition

**Table-2.** Material properties for FE model (Latif *et al.* 2013), (Pawaskar *et al.*, 2010).

| Parameter | Value |
|---|---|
| **Young's Modulus, $E_{cartilage}$** | **0.54 MPa** |
| Poisson's ratio, $v_{cartilage}$ | 0.08 |
| Permeability, $k_{cartilage}$ | 4.0 x 10 $^{-15}$ m$^4$/Ns |
| Young's Modulus, $E_{bone}$ | 2000 MPa |
| Poisson's ratio, $v_{bone}$ | 0.2 |

In order to simulate the creep-deformation phenomenon, a ramp load of 0.38 N was applied on the indenter for 2 s, and the load were then maintained for further 1000 s to reach its equilibrium.

**Validation of finite element model**

The model by previous study was reconstructed by applying the same boundary and interface conditions, element type and cartilage properties to validate the implementation of the contact-dependent flow detection algorithm. The present developed model generated identical contact pressure and pore pressure as compared with Pawaskar (2010) as shown in Figures 4 and 5.

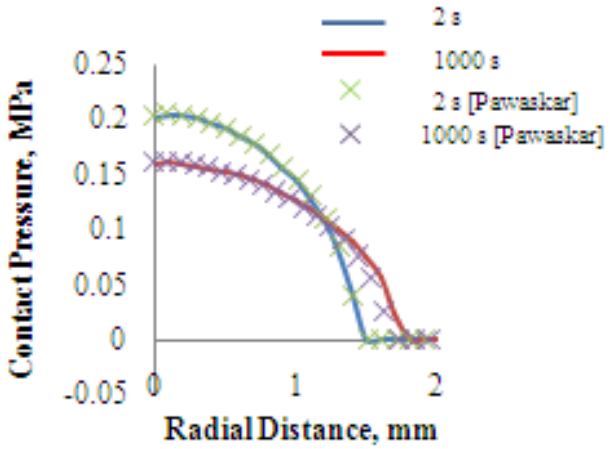


**Figure-4.** Contact pressure distribution at cartilage surface of creep deformation, showing comparison between current study and previous result of Pawaskar (2010).

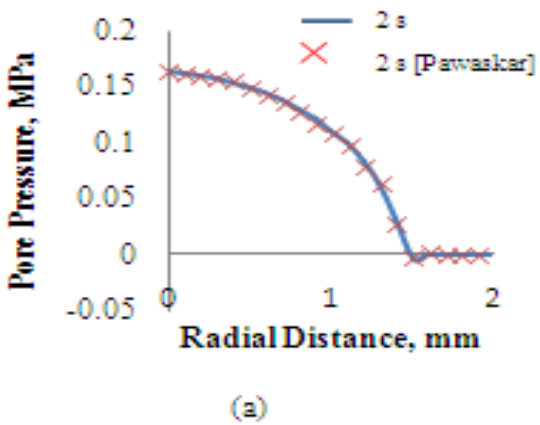


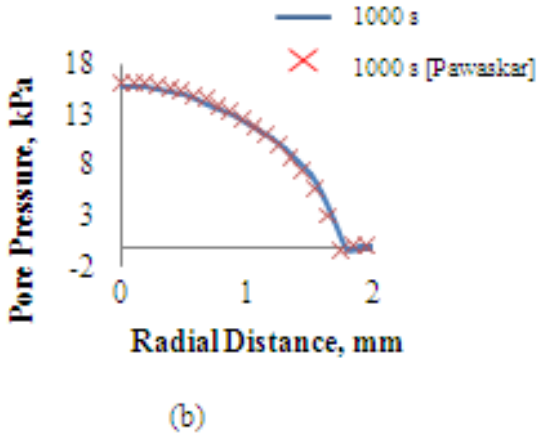


**Figure-5.** Pore pressure distribution at cartilage surface of creep deformation, (a) 2s, (b) 1000s, showing comparison between current study and the previous results of Pawaskar (2010).

**RESULT AND DISCUSSIONS**

The cartilage thickness study was carried out to observe the effect of contact pressure and pore pressure during creep indentation test using axisymmetric FE model. Figures 6 and 7 show the variation in contact pressure and pore pressure for different cartilage thickness.

At 2s it was found that the 0.3 mm cartilage thickness generated 48% higher of the contact pressure compared to 0.7 mm. The trend was similar for 1000s where the percentage difference was 44%. The reduction in contact pressure from 2s to 1000s may be due to the reduction in load at the cartilage-indenter interface.

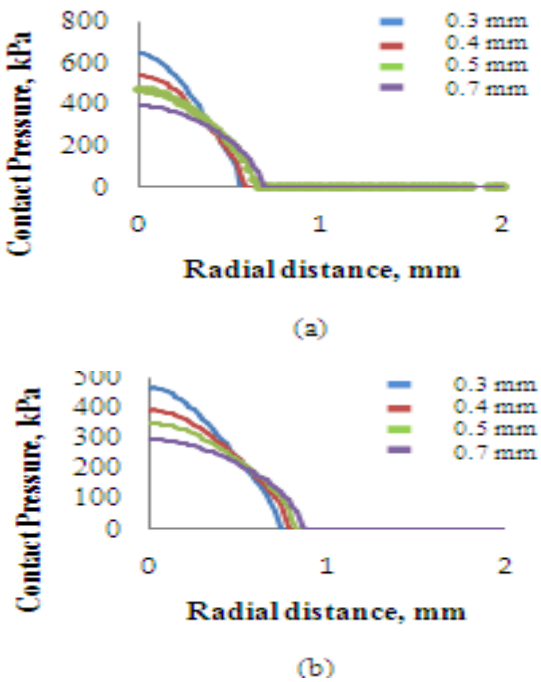


**Figure-6.** Distribution of contact pressure at the cartilage surface for different cartilage thickness after (a) 2s and (b) 1000s.

For the pore pressure, the 0.3 mm cartilage thickness generated 59% higher compared to 0.7 mm at 2s. However, at 1000s the pore pressure of 0.7 mm thickness cartilage is the highest as shown in Figure-7(b).

At 1000s, the pore pressure was dropped drastically as the fluid flow exudation spread towards to the cartilage surface, while at 2s; the direction of fluid flow exudation is concentrated towards the cartilage as can be seen in Figure 8. However, opposite trend was observed at 1000s, where the 0.7 mm thickness generated the highest pore pressure. This could be due to the increased of the interstitial fluid flow in order to maintain the equilibrium.

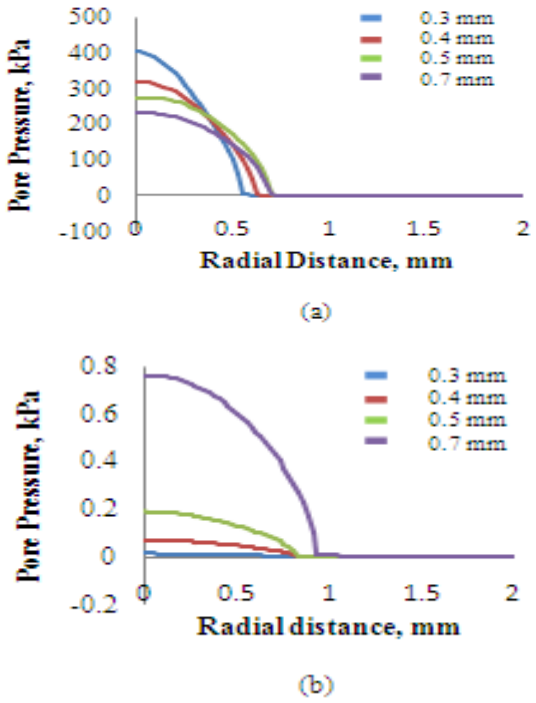


**Figure-7.** Distribution of pore pressure at the cartilage surface for different surface thickness after (a) 2s and (b) 1000s.

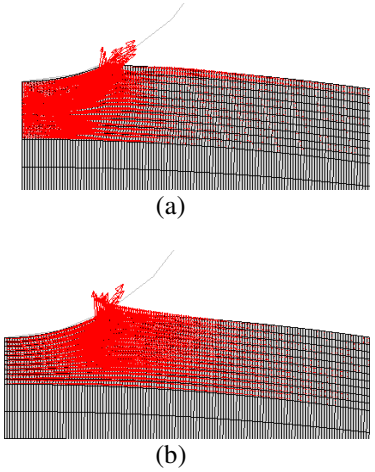


**Figure-8.** Direction of fluid velocity vector at (a) 2s and (b) 1000s.

From the axisymmetric FE model, it show that contact pressure and pore pressure has an important role in cartilage behavior. The prediction of cartilage degeneration can be made as the excessive wear of the cartilage may result from very high contact pressure of cartilage surface. Besides that, the interstitial fluid flow can be determined to know fluid flow exudation from the cartilage tissue. The increasing of interstitial fluid flow out the tissue leads to the surface porosity and increased permeability which caused the surface becomes damaged. It also generate higher percentage of tissue deformation when the matrix is mechanically loaded (Grenier *et al*., 2014). The contact behavior of cartilage tissue provides more understanding about cartilage function and cartilage degeneration. This is in agreement with sensitivity study in FE carried out by Li (2013) and Anderson (2008) who claimed the cartilage thickness is crucial to the contact mechanics behavior and distribution.

## CONCLUSIONS

In the present study, the effects of cartilage thickness to the contact pressure and pore pressure of cartilage in indentation test using axisymmetric FE model were investigated. The assumption by the previous studies that the cartilage has a flat surface and uniform thickness may cause the limitation of the accuracy of the study of the cartilage behavior.

Based on the result, it shows that the thickness does give an effect to the contact mechanics of the cartilage tissue. The cartilage thickness depends on the species, joints, location within joints and edge, thus the material properties of the cartilage vary between individuals. For further studies in effect of the cartilage thickness in characterization of cartilage properties could be studied for better understanding about development of OA.

## ACKNOWLEDGEMENT

This study is funded by the Ministry of Higher Education of Malaysia (MOHE), FRGS (RACE)/2013/ FKM/TK2/1 F00200. The support from the Universiti Teknikal Malaysia Melaka is gratefully acknowledged.

## REFERENCES

Abd Latif, M.J., Jin, Z. and Wilcox, R.K. 2012. Biomechanical characterisation of ovine spinal facet joint cartilage. Journal of Biomechanics, 45(8), pp.1346-1352.

Anderson, A. E., Ellis, B. J., Maas, S. A., Peters, C. L., and Weiss, J. A. 2008. Validation of finite element predictions of cartilage contact pressure in the human hip joint. Journal of Biomechanical Engineering, 130(5), 051008.

Bhosale, A.M. and Richardson, J.B., 2008. Articular cartilage: structure, injuries and review of management. British medical bulletin, 87, pp.77-95.

Boschetti, F., Pennati, G., Gervaso, F., Peretti, G.M. and Dubini, G. 2004. Biomechanical properties of human articular cartilage under compressive loads. Biorheology, 41, pp.159-166.

Buckwalter, J. a and Martin, J. a, 2006. Osteoarthritis. Advanced drug delivery reviews, 58(2), pp. 150-67.

Choi, A.P.C. and Zheng, Y.P. 2005. Estimation of Young's modulus and Poisson's ratio of soft tissue from indentation using two different-sized indentors: Finite element analysis of the finite deformation effect. Medical and Biological Engineering and Computing, 43(2), pp.258-264.

Danso, E.K., Honkanen, J.T.J., Saarakkala, S. and Korhonen, R. K. 2014. Comparison of nonlinear mechanical properties of bovine articular cartilage and meniscus. Journal of Biomechanics, 47(1), pp. 200-206.

Egloff, C., Hügle, T. and Valderrabano, V. 2012. Biomechanics and pathomechanisms of osteoarthritis. Swiss medical weekly, 142.

Grenier, S., Bhargava, M.M. and Torzilli, P. a, 2014. An in vitro model for the pathological degradation of articular cartilage in osteoarthritis. Journal of biomechanics, 47(3), pp. 645-52.

Harris, M.D., Anderson, A.E. and Henak, C.R. 2012. Finite element prediction of cartilage contact stresses in normal human hips. Journal of Orthopaedic Research, 30(7), pp. 1133-1139.

Jurvelin, J.S., Rasanen, T., Kolmonen, P. and Lyyra, T. 1995. Comparison of optical, needle probe and ultrasonic techniques for the measurement of articular cartilage thickness. Journal of Biomechanics, 28(2), pp. 231-235.

Kazemi, M., Dabiri, Y. and Li, L.P. 2013. Recent advances in computational mechanics of the human knee joint. Computational and Mathematical Methods in Medicine, 2013.

Latif, M.J.A., Hashim, N.K., Ramlan, R., Mahmud, J., Jumahat, A. and Kadir, M.R.A. 2013. The Effects of Surface Curvature on Cartilage Behaviour in Indentation Test: A Finite Element Study. Procedia Engineering, 68, pp. 109-115.

Li, J., Stewart, T.D., Jin, Z., Wilcox, R.K. and Fisher, J. 2013. The influence of size, clearance, cartilage properties, thickness and hemiarthroplasty on the contact mechanics of the hip joint with biphasic layers. Journal of Biomechanics, 46(10), pp. 1641-1647.

Matsiko, A., Levingstone, T.J. and O'Brien, F.J. 2013. Advanced strategies for articular cartilage defect repair. Materials, 6, pp. 637-668.

Meng, Q., Zhongmin, J., Fisher, J., and Wilcox, R. 2013. Comparison between FEBio and Abaqus for biphasic contact problems. Proceedings of the Institution of Mechanical Engineers. Part H, Journal of engineering in medicine, 227(9), pp. 1009-19.

Pawaskar, S. S., Fisher, J., and Jin, Z. 2010. Robust and general method for determining surface fluid flow boundary conditions in articular cartilage contact mechanics modeling. Journal of Biomechanical Engineering, 132(3), pp. 031001.

Sharma, C., Gautam, S., Dinda, A.K. and Mishra, N.C. 2011. Cartilage tissue engineering: Current scenario and challenges. Advanced Materials Letters, 2, pp. 90-99.

Shepherd, D.E. and Seedhom, B.B. 1999. Thickness of human articular cartilage in joints of the lower limb. Annals of the rheumatic diseases, 58(1), pp.27-34.

Tchetina, E. V. 2011. Developmental Mechanisms in Articular Cartilage Degradation in Osteoarthritis. Arthritis, 2011, pp. 1-16.

Toyras, J., Laitinen, T.L. and Niinimaski, M. 2001. Estimation of the Young's modulus of articular cartilage using an arthoscopic indentation instrument and ultrasonic measurement of tissue thickness. Journal of Biomechanics, 34, pp. 251-256.